

Past climates inform our future: Review Summary

Jessica E. Tierney, Christopher J. Poulsen, Isabel P. Montañez,
Tripti Bhattacharya, Ran Feng, Heather L. Ford, Bärbel Hönlisch, Gordon N. Inglis,
Sierra V. Petersen, Navjit Sagoo, Clay R. Tabor, Kaustubh Thirumalai, Jiang Zhu,
Natalie J. Burls, Yves Goddérís, Gavin L. Foster, Brian T. Huber, Linda C. Ivany,
Sandra K. Turner, Daniel J. Lunt, Jennifer C. McElwain, Benjamin J. W. Mills,
Bette L. Otto-Bliesner, Andy Ridgwell, Yi Ge Zhang

July 6, 2020

Background: Anthropogenic emissions are rapidly altering Earth’s climate, pushing it toward a warmer state for which there is no historical precedent. Although no perfect analogue exists for such a disruption, Earth’s history includes past climate states – “paleoclimates” – that hold lessons for the future of our warming world. These periods in Earth’s past span a tremendous range of temperatures, precipitation patterns, cryospheric extent, and biospheric adaptations, and are increasingly relevant for improving our understanding of how key elements of the climate system are affected by greenhouse gas levels. The rise of novel geochemical and statistical methods, as well as improvements in paleoclimate modeling, allow for formal evaluation of climate models based on paleoclimate data. In particular, given that some of the newest generation of climate models have a high sensitivity to a doubling of atmospheric CO₂, there is a renewed role for paleoclimates in constraining equilibrium climate sensitivity (ECS) and its dependence on climate background state.

Advances: In the past decade, an increasing number of studies have used paleoclimate temperature and CO₂ estimates to infer ECS in the deep past, in both warm and cold climate states. Recent studies support the paradigm that ECS is strongly state-dependent, rising with increased CO₂ concentrations. Simulations of past warm climates such as the Eocene further highlight the role that cloud feedbacks play in contributing to high ECS under elevated CO₂ levels. Paleoclimates have provided critical constraints on the assessment of future ice sheet stability and concomitant sea level rise, including the viability of threshold processes like marine ice cliff instability. Beyond global-scale changes, analysis of past changes in the water cycle have advanced our understanding of dynamical drivers of hydroclimate, which is highly relevant for regional climate projections and societal impacts. New and expanding techniques, such as analyses of single shells of foraminifera, are yielding sub-seasonal climate information that can be used to study how intra- and interannual modes of variability are affected by external climate forcing. Studies of extraordinary, transient departures in paleoclimate from the background state such as the Paleocene-Eocene Thermal Maximum provide critical context for the current, anthropogenic aberration, its impact on the Earth system, and the timescale of recovery.

A number of advances have eroded the “language barrier” between climate model and proxy data, facilitating more direct use of paleoclimate information to constrain model performance. It is increasingly common to incorporate geochemical tracers – such as water isotopes – directly into model simulations and this practice has vastly improved model – proxy comparisons. The development of new statistical approaches rooted in Bayesian inference has led to a more thorough quantification of paleoclimate data uncertainties. Finally, techniques like data assimilation allow for a formal combination of proxy and model data into hybrid products. Such syntheses provide a full-field view of past climates and can put constraints on climate variables that we have no direct proxies for, such as cloud cover or wind speed.

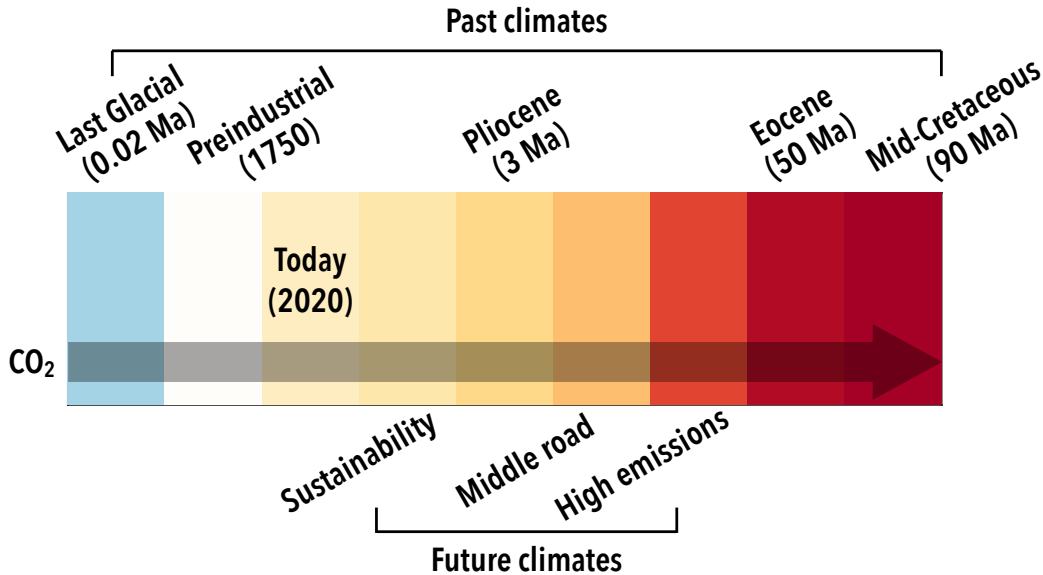


Figure 1: Past climates (denoted on top) provide context for future climate scenarios (at bottom). Ma = millions of years ago. Both past and future climates are colored by their estimated change in global mean annual surface temperature relative to preindustrial conditions. “Sustainability”, “Middle road”, and “High emissions” represent the estimated global temperature anomalies at 2300 from the Shared Socioeconomic Pathways (SSPs) SSP1-2.6, SSP2-4.5, and SSP5-8.5, respectively. In both the past and future cases, warmer climates are associated with increases in CO₂.

Outlook: A common concern with using paleoclimate information as model targets is that non-CO₂ forcings, such as aerosols and trace greenhouse gases, are not well known, especially in the distant past. While evidence thus far suggests that such forcings are secondary to CO₂, future improvements in both geochemical proxies and modeling are on track to tackle this issue. New and rapidly evolving geochemical techniques have potential to provide improved constraints on the terrestrial biosphere, aerosols, and trace gases; likewise, biogeochemical cycles can now be incorporated into paleoclimate model simulations. Beyond constraining forcings, it is critical that proxy information is transformed into quantitative estimates that account for uncertainties in the proxy system. Statistical tools have already been developed to achieve this, which should make it easier to create robust targets for model evaluation. With this increase in quantification of paleoclimate information, we suggest that modeling centers include simulation of past climates in their evaluation and statement of their model performance. This practice is likely to narrow uncertainties surrounding climate sensitivity, ice sheets, and the water cycle and thus improve future climate projections.

Past climates inform our future

Jessica E. Tierney,^{1*} Christopher J. Poulsen,² Isabel P. Montañez,³
Tripti Bhattacharya,⁴ Ran Feng,⁵ Heather L. Ford,⁶ Bärbel Hönlisch,⁷ Gordon N. Inglis,⁸
Sierra V. Petersen,² Navjit Sagoo,⁹ Clay R. Tabor,⁵ Kaustubh Thirumalai,¹ Jiang Zhu,²
Natalie J. Burls,¹⁰ Gavin L. Foster,⁸ Yves Goddérès,¹¹ Brian T. Huber,¹² Linda C. Ivany,⁴
Sandra K. Turner,¹³ Daniel J. Lunt,¹⁴ Jennifer C. McElwain,¹⁵ Benjamin J. W. Mills,¹⁶
Bette L. Otto-Bliesner,¹⁷ Andy Ridgwell,¹³ Yi Ge Zhang¹⁸

¹Department of Geosciences, University of Arizona

²Department of Earth and Environmental Sciences, University of Michigan

³Department of Earth and Planetary Sciences, University of California, Davis

⁴Department of Earth Sciences, Syracuse University

⁵Department of Geosciences, University of Connecticut

⁶School of Geography, Queen Mary University of London

⁷Lamont-Doherty Earth Observatory and the Department of Earth and Environmental Sciences, Columbia University

⁸School of Ocean and Earth Science, National Oceanography Centre Southampton, University of Southampton

⁹Department of Meteorology, University of Stockholm

¹⁰Department of Atmospheric, Oceanic, and Earth Sciences, George Mason University

¹¹Centre National de la Recherche Scientifique, Géosciences Environnement Toulouse

¹²Department of Paleobiology, National Museum of Natural History

¹³Department of Earth Science, University of California, Riverside

¹⁴School of Geographical Sciences, University of Bristol

¹⁵Department of Botany, Trinity College Dublin

¹⁶School of Earth and Environment, University of Leeds

¹⁷National Center for Atmospheric Research

¹⁸Department of Oceanography, Texas A&M University

*Corresponding Author

July 6, 2020

1 **As the world warms, there is a profound need to improve projections**
2 **of climate change. While the latest Earth system models offer an un-**
3 **precedented number of features, fundamental uncertainties continue to**
4 **cloud our view of the future. Past climates provide the only opportu-**
5 **nity to observe how the Earth system responds to high CO₂, underlining**
6 **a fundamental role for paleoclimatology in constraining future climate**
7 **change. Here, we review the relevancy of paleoclimate information for**
8 **climate prediction and discuss the prospects for emerging methodologies**
9 **to further insights gained from past climates. Advances in proxy methods**

10 **and interpretations pave the way for the use of past climates for model**
11 **evaluation – a practice we argue should be widely adopted.**

12 **1 Introduction**

13 The discipline of paleoclimatology is rooted in the peculiarities of the geological record, which has
14 long hinted that Earth’s climate can change in profound ways. In possibly the first paleoclimate
15 study, the 17th century English physicist Robert Hooke concluded, based on observations of
16 large turtles and ammonites in Jurassic rocks, that conditions in England had once been much
17 warmer than now (1). Since then, paleoclimate studies have revolutionized our view of the
18 climate system (2), documenting both warm and cold worlds much different than the one we
19 inhabit, and establishing the link between atmospheric CO₂ and global temperature (Fig. 1).

20 While paleoclimatology continues to narrate the history of Earth’s climate, it also plays an
21 increasingly central role in understanding future climate change. The study of past climate has
22 never been more relevant than now, as anthropogenic activities increase atmospheric greenhouse
23 gas concentrations and modify the land surface and ocean chemistry at a rate and scale that
24 exceed natural geologic processes. CO₂ levels are higher now than at any point in at least the
25 last three million years and, at the current rate of emissions, will exceed concentrations typical
26 of the last 30 million years by 2300 (Fig. 1). In this context, past climates are windows into
27 our future (3) – the geological record is the only observational source of information for how the
28 climate system operates in a state much warmer than the present.

29 The challenge for paleoclimatology is that there are few direct quantitative records of past
30 climate (e.g. temperature, precipitation). Instead, we make use of “proxies,” surrogates for
31 climate variables that cannot be measured directly. In some cases, the physical occurrence
32 (or absence) of a proxy (like glacial deposits) reveals information about past environmental
33 conditions. More often, geochemical data (such as elemental and stable isotope ratios) stored in
34 fossils, minerals, or organic compounds, are used to infer past conditions. The discovery of new
35 proxies, improvements in modeling and analytical techniques, and the increasing number of proxy
36 records are actively expanding the utility of paleoclimate information. These innovations are
37 refining our understanding of how the climate system responds to large changes in atmospheric
38 CO₂, and provide insights into aspects of past climates (such as seasonality and interannual
39 variability) that were heretofore unknowable.

40 Among the most important contributions that paleoclimatology can make is the evaluation
41 of Earth system models that we rely on for projecting future climate change. The physical
42 parameterizations in these sophisticated models are often tuned to fit the preindustrial or his-
43 torical record (4). However, the latter is short in duration and samples a single climate state
44 with a narrow CO₂ range. The performance of climate models under extreme forcing very
45 different than present is not commonly assessed, despite the fact that the models are used to
46 project changes under high-emissions scenarios. When these models are used to simulate past
47 warm climates, they often predict surface temperatures that are too cold and pole-to-equator
48 temperature gradients that are too large (5). However, a new generation of models, alongside
49 developments in proxy techniques and analysis, now provide opportunities to more fully exploit
50 past climates for model evaluation and assessment of key metrics of the climate system.

51 2 Past climates inform key processes

52 Earth’s paleoclimate record contains tremendous variability. Over the last 100 million years, the
53 climate gradually transitioned from an ice-free world of exceptional warmth (the mid-Cretaceous,
54 92 Ma, Fig. 1) to the cold ice ages of the past few million years, glacial worlds with kilometers-
55 thick ice caps covering one-fourth of the land surface (such as the Last Glacial Maximum (LGM),
56 21 ka, Fig. 1). Between Cretaceous and LGM extremes lie intermediate warm climates such as
57 the early Eocene (53–49 Ma) and Pliocene (5.3–2.6 Ma) (Fig. 1). This long-term climate transi-
58 tion was far from steady – short-lived hyperthermal events (6) and cold stadials (7) punctuated
59 the slower trends.

60 Atmospheric CO₂ concentrations generally follow these swings in global temperature (Fig. 1).
61 Geochemical modeling demonstrates that the balance of geological sources (degassing through
62 volcanism) and sinks (weathering and sedimentation) explains the general features of CO₂’s
63 trajectory (8) and establishes causality – high CO₂ leads to high temperatures. The apparent
64 exceptions to this rule, including the end-Cretaceous and early Paleocene (70–60 Ma) and the
65 Miocene (23–5.3 Ma), are areas of active research. One explanation for the decoupling of CO₂
66 and temperature is that uncertainties associated with the proxies blur the relationship. Esti-
67 mation of past CO₂ is challenging. Beyond the ice core record (9), CO₂ information comes
68 from geochemical data, such as isotope ratios of boron and carbon, or paleobotanical indicators
69 such as the density of leaf stomata. All of these proxies require assumptions about the phys-
70 ical, chemical, and biological state of the past that are not completely understood, sometimes
71 leading to misinterpretations of the signal (10). Proxy methodologies and assumptions continue
72 to be refined, and there is some indication that CO₂ at the end of the Cretaceous may have
73 been higher than shown in Fig. 1 (11). It is also possible that these discrepancies have another
74 explanation, such as a greater-than-expected role for non-CO₂ forcings and feedbacks. If the
75 paleoclimate record has taught us anything, it is that the more we probe, the more we learn.

76 Past climate states were profoundly different from today. Their global mean temperatures,
77 latitudinal temperature gradients, polar ice extents, regions of deep-water formation, vegetation
78 types, patterns of precipitation and evaporation, and variability were all different. These dif-
79 ferences are invaluable as they provide rich evidence of how climate processes operated across
80 states that span the range of CO₂ concentrations (400–2000 ppm) associated with future emis-
81 sions scenarios (the Shared Socioeconomic Pathways (SSPs), Fig. 1). Under the sustainable
82 SSP1-2.6 scenario, in which emissions are curtailed and become net-negative by the end of the
83 21st century, CO₂ concentrations would be stabilized near Pliocene levels (Fig. 1). In contrast,
84 under the fossil-fuel intensive SSP5-8.5 scenario, CO₂ concentrations would approach or even
85 exceed Eocene or mid-Cretaceous levels (Fig. 1). These past warm climates therefore serve as
86 targets against which to measure the increasingly complex generation of climate models that
87 are used for future climate prediction.

88 Past climates are not perfect analogues for future states – continental configurations are
89 increasingly different with age, and they often represent equilibrium climates as opposed to
90 transient changes associated with rapid greenhouse gas emissions (12). But as benchmarks for
91 climate models, ancient climates need not be perfect analogues. In fact, the differences are
92 advantageous; they provide true out-of-sample validation for the strength and stability of key
93 feedbacks; large-scale responses of the hydrological cycle; and the most ubiquitous metric of all,

94 climate sensitivity.

95 **3 Paleoclimate constraints on climate sensitivity**

96 Equilibrium climate sensitivity (ECS) has been widely adopted as a simple metric of how re-
97 sponsive the Earth’s climate system is to radiative forcing. It is defined as the change in global
98 near-surface air temperature resulting from a sustained doubling in atmospheric CO₂ after the
99 fast-acting (timescales of years to decades) feedback processes (water vapor, clouds, snow) in
100 the Earth system reach equilibrium. The 5th assessment report of the IPCC determined that
101 ECS was likely between 1.5 and 4.5°C, a large range that has remained essentially unchanged for
102 40 years (13). Because the environmental impacts, socio-economic implications, and mitigation
103 timescales are very different for a low versus a high ECS (14), narrowing its range has always
104 been a high priority.

105 The fact that models with either a low or high present-day ECS can match historical ob-
106 servations (15) suggests that preindustrial and industrial climatic changes provide insufficient
107 constraints on this important metric. Furthermore, the emerging view is that ECS is depen-
108 dent on, and changes with, the background climate state – specifically, it increases in warmer
109 climates (16–19). Past warm climates therefore provide key constraints on the range of plausi-
110 ble ECS values as well as the strength of feedbacks involved. Simulations of the early Eocene
111 provide a salient example. Figure 2 shows a comparison between the ECS of Coupled Model In-
112 tercomparison Project (CMIP) Phase 5 and Phase 6 models (used in the last and the upcoming
113 IPCC assessments) and the ECS of preindustrial and Eocene simulations conducted with the
114 National Center for Atmospheric Research (NCAR) Community Earth System Model (CESM)
115 version 1.2 (19). Doubling CO₂ in an Eocene experiment with preindustrial CO₂ (285 ppm;
116 1X) yields an ECS similar to the preindustrial experiment and overlaps with the CMIP range
117 (Fig. 2). This indicates that non-CO₂ Eocene boundary conditions, including the position of
118 the continents and the absence of continental ice sheets, do not have a large effect on ECS in
119 CESM1.2. In contrast, raising CO₂ levels elevates ECS in the Eocene simulations to values above
120 6°C (Fig. 2). This increase in ECS with increasing temperature results in accurate simulation
121 of Eocene temperatures at CO₂ concentrations that agree with proxy estimates (Fig. 2, inset).
122 The elevated ECS under high CO₂ in CESM1.2 is due to improved representation of clouds in
123 the CAM5 atmospheric model, which drives a strong low-cloud positive feedback under high
124 CO₂ (19) – a finding in agreement with the emerging recognition that cloud feedbacks are a
125 key component of warm climates (20, 21). The fact that CESM1.2 simulates Eocene proxy tem-
126 peratures within the bounds of proxy CO₂ estimates provides support for its cloud physics and
127 increases our confidence in the model’s state-dependent ECS. The Geophysical Fluid Dynamics
128 Laboratory (GFDL) CM2.1 model can also simulate the large-scale features of Eocene proxy
129 temperatures (22), likewise suggesting that its ECS is reasonable. On the other hand, CESM2
130 (the newest version of the NCAR model) estimates Eocene temperatures that exceed the upper
131 bound of proxy constraints at low CO₂ levels (23), suggesting that its modern ECS of 5.3°C
132 is too high. A little more than a third of the newest-generation CMIP6 models have an ECS
133 higher than 4.5°C (15). From historical observations alone, it is very challenging to assess the
134 plausibility of these higher ECS values. As the Eocene example highlights, warm paleoclimates
135 are key in this respect.

136 The early Eocene provides an important constraint on model ECS but samples a single
137 high-CO₂ climate state. Given the dependence of ECS on the background climate state, other
138 past climates are critical to constraining ECS and relevant physics under both lower (e.g. LGM,
139 Pliocene) and higher (e.g. Eocene, Cretaceous) background CO₂ levels. One concern about using
140 past climates as model targets is that the forcings, especially aerosol and non-CO₂ greenhouse
141 gas concentrations, are uncertain and increasingly so in the distant past. While important, it is
142 worth noting that these forcings are secondary to CO₂ (e.g. (24)) and, for extreme climates like
143 the Eocene and Cretaceous, may largely fall within the climate proxy uncertainties. Moreover,
144 this concern can be mitigated by examining model responses to the potential range of under-
145 constrained forcings and, as is increasingly done, by incorporating biogeochemical cycles and
146 the simulation of aerosol production and transport into the models.

147 4 Paleoclimate perspectives on the stability of the cryosphere

148 Future projections of sea level rise have large uncertainties, mainly due to unknowns surrounding
149 the stability and threshold behavior of ice sheets (25). The paleoclimate record furnishes true
150 “out-of-sample” tests for understanding the sensitivity of the cryosphere to warming that can
151 lower these uncertainties. The past few years have seen a number of advances on both data
152 and climate modeling fronts to understand past changes in ice sheets and connect these to the
153 future. Advances in the generation and interpretation of proxy indicators of ice sheet size, shape,
154 and extent (26–28) are helping to refine our understanding of cryosphere dynamics in warmer
155 climates. Improvements in modeling the effects of dynamic topography and glacial isostatic
156 adjustment are continually reducing uncertainties associated with estimates of past global sea
157 level (29, 30), providing more accurate benchmarks for model simulations (31).

158 Paleoclimates also provide critical insights into processes that drive destabilization of ice
159 sheets. Of particular relevance for future projections is assessing the likelihood of marine ice-
160 cliff instability (MICI), a rapid collapse of coastal ice cliffs following the disintegration of an
161 ice shelf, which has the potential to contribute to substantial sea level rise by the end of the
162 21st century (32, 33). The record of sea level change from past warm climates offers a way to
163 test this hypothesis. Recent work has focused on the Pliocene, given that CO₂ concentrations
164 during this time were similar to current anthropogenic levels (Fig. 1). A new reconstruction of
165 global mean sea-level during the mid-Pliocene warm period indicates a rise of ~ 17 m, implying
166 near-to-complete loss of Greenland and the West Antarctic Ice Sheet with some additional
167 contribution from East Antarctica (34). While this represents an outstanding loss of ice, MICI
168 is not necessarily needed to explain it (33, 34). However, simulated changes in sea level are highly
169 dependent on each model’s treatment of ice sheet stability (35), and paleoclimate investigations
170 of warmer climates, such as the early Pliocene and the Miocene, indicate larger magnitudes of
171 ice loss, thermal expansion, and consequent sea level rise (34, 36). Moving forward, refining our
172 understanding of threshold behavior in ice sheets, and thus improving projections of future sea
173 level rise, will require a synergistic approach that leverages paleoclimate estimates from multiple
174 warm climates alongside solid Earth, ice sheet, and climate modeling (31).

5 Regional and seasonal information from past climates

Future warming will shift regional and seasonal patterns of rainfall and temperature, with dramatic consequences for human society (37, 38). Regional changes in the land surface (reduced snow cover, melting permafrost, greening, desertification) can further trigger biogeochemical feedbacks that could dampen or amplify initial radiative forcing, with implications for climate sensitivity (39). Unfortunately, climate models disagree about the direction and magnitude of future regional rainfall change (40). Improving future predictions of regional climate requires separating internal variability in the climate system (i.e., interannual–centennial oscillations) from externally-forced changes (i.e., from greenhouse gases or aerosols). Regional and seasonal paleoclimate data are critical in this respect, as they provide long, continuous estimates of the natural range of variation, augmenting the relatively short observational record (41, 42).

Subannually-resolved paleobiological and sedimentary archives, made more accessible by recent advances in geochemical techniques, allow for the study of seasonal-scale variations in both temperature and hydroclimate. For example, $\delta^{18}\text{O}$ measurements of fossil bivalves can be used to gain insights into the drivers of seasonal variability during the Eocene greenhouse climate (43, 44) (Fig. 3a). Since individual planktic foraminifera live for about a month, analyses of single shells yields subannual sea-surface temperature (SST) data from ancient climates (45). This can be leveraged to reveal past changes in key seasonal phenomena such as the El Niño–Southern Oscillation (ENSO) (46) (Fig. 3). Proxy data can even provide records of changes in the frequency or intensity of extreme events like hurricanes (47).

Reconstructions of hydroclimate are considerably more challenging than temperature, as proxy signals tend to be more complex; however, even basic directional information (wetter vs. drier) can be used to test spatial patterns in models (e.g., (48)). Past warm climates allow us to test the extent to which the thermodynamic “wet-gets-wetter, dry-gets-drier” response broadly holds with warming (49) or if dynamical changes, such as shifts in the Hadley or Walker cells, play more of a key role in the regional water cycle response to changes in surface temperature gradients (48, 50).

Comparisons of proxies and models can also be used to identify the processes that are critical for accurate simulation of regional shifts in the water cycle, where local moisture and energy budgets exert an important control (51). The processes that drive these budgets – i.e., land surface properties and clouds – must be parameterized in global climate models and are often poorly understood, yet have huge consequences for predicted patterns in humidity and rainfall (52–55). Past changes in Earth’s boundary conditions offer a much broader set of scenarios where observations can be used to evaluate the performance of parameterization schemes. In particular, paleoclimates spanning the last glacial cycle have helped us better understand the role of land-atmosphere feedbacks in determining hydroclimatic response. Analyses of LGM proxies for SST and water balance in Southeast Asia suggest a direct relationship between convective parameterization and model skill at capturing regional hydroclimate (48, 56). Studies of the mid-Holocene ‘Green Sahara’ highlight the importance of vegetation and dust feedbacks in accurately simulating the response of the west African monsoon to radiative forcing (57, 58). These examples demonstrate the value of hydroclimate proxy-model comparison even if the past climate state is not a direct analogue for future warming.

Studies of past warm climates have the potential to provide even more insights into the

218 behavior of regional climate in a warming world. Future model projections broadly simulate a
219 pattern of subtropical drying, while the deep tropics and high latitudes get wetter (40). Recently,
220 however, researchers have argued that subtropical drying is transient and might not persist in
221 equilibrium with higher radiative forcing (59, 60). Indeed, several paleoclimatic intervals (61, 62)
222 suggest that a warmer world could feature a different pattern, with wetter conditions in both the
223 subtropics and high latitudes (50). This pattern is especially evident in western North America,
224 where widespread Pliocene lake deposits suggest much wetter conditions (63). This evidence
225 stands in stark contrast to future projections for this region, which overwhelmingly predict drier
226 conditions and more intense droughts (64), and suggests that paleoclimates can provide vital
227 constraints on the response of arid lands to higher CO₂ concentrations.

228 6 Climatic aberrations

229 Among the most important discoveries in paleoclimatology is the occurrence of climatic “aber-
230 rations” – extraordinary transient departures from a background climate state. Such events are
231 distinguished by radical changes in temperature, precipitation patterns, and ocean circulation
232 that often leave distinctive marks in the geological record, like the pervasive black shales of
233 the mid-Cretaceous Ocean Anoxic Events (65). An aberration typically occurs in response to
234 a short-lived perturbation to the climate system, such as a sudden release of greenhouse gases
235 (e.g., from volcanoes, methane clathrates, or terrestrial organic deposits). Aberrations need not
236 be “abrupt” in the sense that the rate of climate change must exceed the rate of forcing, and
237 they can potentially last for a long time (for example, the Sturtian Snowball Earth lasted 55
238 million years (66)). They are instructive because they provide information on extreme climate
239 states, and the ability of the Earth system to recover from such states.

240 One of the most striking aberrations in the paleoclimate record, the Paleocene-Eocene Ther-
241 mal Maximum (PETM), may foreshadow future changes that Earth will experience due to
242 anthropogenic emissions. The PETM, which occurred 56 million years ago, was triggered by
243 rapid emission of greenhouse gases; proxy and model estimates suggest that CO₂ doubled or
244 even tripled from a background state of ~900 ppm (67–69) in less than 5,000 years (70, 71). In
245 response, global temperatures spiked by 4–6°C (72). The surface ocean rapidly acidified (68, 73),
246 and seafloor carbonates dissolved (74), resulting in dramatic biogeographic range shifts in plank-
247 ton and the largest extinction in deep-sea calcifying benthic foraminifera ever observed (75). Pre-
248 cipitation patterns changed dramatically, with much more rain falling at the high latitudes (76).
249 It took the Earth ~ 100,000 years to recover from this perturbation (68, 77).

250 Although the PETM stands out starkly in the geologic record, the rate of CO₂ release was still
251 4–10 times slower than current anthropogenic emissions (71, 78). Indeed, the geological record
252 leaves no doubt that our current rate of global warming, driven by anomalous (anthropogenic)
253 forcing, is an exceptional aberration – the rate and magnitude of change far exceeds the typical
254 multi-thousand year variability that preceded it (Fig. 4). In the last 100 million years, CO₂
255 has ranged from maximum values in the mid-Cretaceous to minimum levels at the Last Glacial
256 Maximum (Fig. 1). Going forward, we are on pace to experience an equivalent magnitude
257 of change in atmospheric CO₂ concentrations, in reverse, over a period of time that is over
258 10,000 times shorter (Fig. 4). In just over 150 years, we have already raised CO₂ concentrations
259 (currently at 410 ppm) to Pliocene levels (Fig. 4). Under a middle-of-the-road emissions scenario

260 such as SSP2-4.5 (or the CMIP5 equivalent, RCP4.5), CO₂ will approach 600 ppm by Year 2100,
261 and if we follow the high-emissions SSP5-8.5 (or RCP8.5), CO₂ will rise beyond mid-Cretaceous
262 concentrations (ca. 1000 ppm) by Year 2100 (Fig. 4). In comparison, over the past 800,000
263 years of geologic history CO₂ only varied between 180 and 280 ppm (9) (see also Fig. 4).

264 How long will it take for the Earth to neutralize anthropogenic CO₂ and return to pre-
265 industrial levels? The Earth has the ability to recover from a rapid increase in atmospheric CO₂
266 concentration – the PETM is a textbook example of this process. In fact, in every case of past
267 CO₂ perturbations, the Earth system has compensated in order to avoid a runaway greenhouse
268 or a permanent icehouse. Yet the natural recovery from aberrations takes place on geological, not
269 anthropogenic, timescales (Fig. 4). Some of the processes that remove CO₂ from the atmosphere
270 occur on relatively short (100–1000 yr) timescales (e.g. ocean uptake), but others take tens to
271 hundreds of thousands of years (e.g. weathering of silicate rocks) (79). Using the intermediate
272 complexity Earth system model cGENIE, we can estimate how long the recovery process takes
273 under different future forcing scenarios. Under an aggressive mitigation scenario (RCP 2.6), CO₂
274 concentrations remain at Pliocene-like concentrations (>350 ppm) through Year 2350, but it still
275 takes hundreds of thousands of years for concentrations to return to preindustrial levels (Fig. 4).
276 Under a middle-of-the-road scenario (RCP 4.5), CO₂ peaks around 550 ppm and remains above
277 Pliocene levels for 30,000 years. Under a worst-case scenario (RCP 8.5) atmospheric CO₂ will
278 remain at mid-Cretaceous (>1000 ppm) concentrations for 5,000 years, at Eocene concentrations
279 (~850 ppm) for 10,000 years, and at Pliocene concentrations (>350 ppm) for 300,000 years (Fig.
280 4). It will be at least 500,000 years, a duration equivalent to 20,000 human generations, before
281 atmospheric CO₂ fully returns to preindustrial levels. Our planet will recover, but for humans,
282 and the organisms with which we share this planet, the changes in climate will appear to be a
283 permanent state shift.

284 7 Bridging the gap between paleoclimate data and models

285 Climate models provide direct estimates of quantities like temperatures, wind speed, and precip-
286 itation. In contrast, paleoclimate information is indirect, filtered through a proxy – a physical,
287 chemical, and/or biological entity that responds to climate – such as foraminifera, algae, or
288 the chemical composition of sediments. Proxies are imperfect recorders of climate; they have
289 inherent uncertainties associated with, for example, biological processes and preservation. Thus,
290 while proxy data can be transformed into climate variables for direct comparison with models
291 using regression, transfer functions, and assumptions, if these structural uncertainties are not
292 accounted for they can lead to unclear or erroneous interpretations. This creates a “language
293 barrier” between model output and proxy data that has limited the use of paleoclimate infor-
294 mation to infer past climate states and evaluate climate models. Three key innovations are
295 now breaking down this barrier, allowing paleoclimate information to directly constrain model
296 performance: 1) the inclusion of chemical tracers relevant to proxies directly in Earth system
297 models; 2) the creation of robust proxy system models that explicitly encode processes, uncer-
298 tainties, and multivariate sensitivities; and 3) the development of statistical methods to formally
299 combine proxy and model data.

300 As far as chemical tracers are concerned, the single most important advance has been the
301 increasingly routine incorporation of water isotopes in model simulations. The stable isotopes

302 of water – $\delta^{18}\text{O}$ and δD – and their incorporation into natural archives are the foundation of
303 modern paleoclimatology (80). A large number of paleoclimate proxies record water isotopes,
304 including foraminifera, stalagmites, leaf waxes, soil carbonates, and ice cores. Water isotope
305 composition, however, reflects multiple processes including changes in temperature, moisture
306 source, evaporation, precipitation, and convection. Including water isotopes in models gener-
307 ates simulated isotope fields that are consistent with the model’s treatment of these processes,
308 eliminating the need to independently conjecture how these various factors may have influenced
309 the proxy data. This creates an “apples to apples” comparison between proxy information and
310 model output that can be used to evaluate model performance and diagnose climatic processes
311 (e.g. (81). For example, using the water-isotope-enabled CESM1.2 (iCESM) (82), it is possi-
312 ble to directly compare carbonate $\delta^{18}\text{O}$ data from Eocene fossil bivalves to model-simulated
313 $\delta^{18}\text{O}$ (43, 44, 83) (Fig. 3a). The model predicts a roughly 3‰ annual range in carbonate $\delta^{18}\text{O}$,
314 in good agreement with observed proxy data (Fig. 3a). The match with the $\delta^{18}\text{O}$ data builds
315 confidence that the model can correctly simulate climatology in this location, and allows us to
316 deconvolve the contribution of SST and $\delta^{18}\text{O}$ of seawater. The site-specific seasonality in SST is
317 8–10°C, while $\delta^{18}\text{O}$ -seawater has a seasonal range of 0.6–0.8‰. This indicates that temperature
318 is primarily responsible for the large seasonal range in carbonate $\delta^{18}\text{O}$ during this greenhouse
319 climate state.

320 One aspect of paleoclimate information that has traditionally limited its use in model eval-
321 uation is an inability to precisely quantify uncertainties surrounding the proxies. However, in
322 the last decade, increasingly detailed proxy system models (84) have been developed to address
323 this issue (e.g.,) (85–87). Many of these use Bayesian inference to quantify uncertainties in the
324 sensitivity of proxies to environmental parameters, which can then be used for probabilistic as-
325 sessments of past climate states, model-proxy agreement, and model evaluation (88). These have
326 helped to transform proxy-model comparisons from qualitative statements (“they look similar”)
327 to quantitative statements (“there is a 90% probability that the data and the model agree”).

328 A final component of the “language barrier” is the fact that proxy data are sparse in both
329 space and time, because they are fundamentally dependent on the presence and preservation
330 of their archives. Yet proxy data are real-world estimates of the “true” climate state. In
331 contrast, climate model information is spatially and temporally continuous and physically self-
332 consistent – but is only a best “guess” at what did or what will happen. One solution to
333 bridge these fundamentally different pieces of information is to formally combine them in a
334 statistical framework and thus leverage their respective strengths. Reduced space methods –
335 commonly used to produce historical reconstructions of climate – can be used to infill missing
336 data and produce maps of paleoclimate states (88, 89). Recently, weather-based data assimilation
337 techniques have been adapted for paleoclimate applications (90). The resulting products are
338 spatially-complete reconstructions of multiple climate variables that represent a balance between
339 the proxy information and the physics and covariance structure of the climate model. This allows
340 local paleoclimate proxy information to be used to infer global metrics of climate – such as global
341 mean air temperature (91). It also allows for the recovery of climatic variables that are consistent
342 with the proxy information but for which we have no direct proxies, such as cloud cover, wind
343 patterns, or precipitation (Fig. 5).

344 In sum, the disintegration of the model-proxy language barrier has narrowed uncertainties
345 in proxy interpretation. Recent studies have been able to use proxy data to infer key cli-

346 matic processes and evaluate models across multiple time periods, including the LGM (*91*), the
347 Pliocene (*88*), and the Eocene (*19, 22*). This opens the door for explicit use of paleoclimates to
348 assess and improve model physics.

349 8 Moving Forward

350 Past climates will continue to provide insights into the range, rate, and dynamics of climate
351 change. Over the last decade, we have witnessed breakthroughs in proxy development and
352 refinement as well as the generation of many new high-resolution marine and terrestrial paleo-
353 oclimate records. In addition to continued advances, the collection of additional temperature
354 and CO₂ proxy records at higher resolution will be paramount for developing better estimates
355 of climate sensitivity. Future proxy collection efforts should also focus on hydroclimate proxies,
356 given the large spread in model projections (*40*). These reconstructions will help us refine our
357 understanding of the response of atmospheric circulation and rainfall to climate change.

358 On the modeling side, the inclusion of chemical tracers, such as water and carbon isotopes,
359 within many of the newly developed CMIP6 (*92*) models offers more robust means of data-model
360 comparison. With these new model tools, we anticipate the rapid development and improvement
361 of data-model synthesis products (*90, 91*) and more focused proxy collection efforts to help
362 reduce model uncertainties. In addition, evaluating CMIP6 models using both the historical and
363 paleoclimate record will result in a more comprehensive and robust approach to understanding
364 the climate system (*93*). We recommend widespread adoption of this practice, so that model
365 ECS and other emergent properties are constrained by paleoclimate data as well as observations.
366 We suggest that weighting or ranking models that perform well over multiple past climate states
367 is a crucial way to constrain the response of the model to changing background conditions and
368 the validity of simulated climate changes under various emissions scenarios. In general, climate
369 models should be able to accurately simulate multiple extreme paleoclimate states – warm and
370 cold – before being trusted for future climate projection.

371 Despite promising CMIP6 model advances, maintaining a variety of models with different
372 levels of complexity is important. Not all climate questions require high levels of model com-
373 plexity, and sometimes complexity is so great that interpretation becomes limited (*94*). In
374 paleoclimatology, complexity can also lead to prohibitive computational expense. Maintained
375 support for lower resolution and variable resolution configurations is vital for better interpreting
376 model results and performing long, transient simulations that can address fundamental questions
377 in paleoclimatology such as glacial cycles and carbon cycle changes.

378 Looking ahead, there are many outstanding process-based uncertainties associated with fu-
379 ture climate change that paleoclimatology can help constrain. For example, paleobotanical
380 records can inform plant physiological responses to changes in CO₂ (*95*), which remain highly
381 uncertain (*96*) but important for quantifying evapotranspirative and surface runoff fluxes. Sim-
382 ilarly, past vegetation reconstructions can assess dynamic vegetation models and simulated
383 changes in the hydrologic cycle through time (*97*). Moreover, additional quantitative reconstruc-
384 tions of hydroclimate, in combination with better constraints on plant physiological functioning
385 in the past, will help refine our understanding of the regional water cycle and its dependence on
386 local energy fluxes and large-scale circulation.

387 New geochemical techniques will also refine our understanding of the Earth system. Devel-

388 opment of radiation (98), biogenic aerosol (99), and dust (100) records have the potential to
389 help constrain past aerosol and cloud radiative effects, which are arguably the most uncertain
390 component of Earth system models (101). In addition, new geochemical tracers for methane
391 cycling (102) and upwelling, which is important for N₂O production (103), will provide unique
392 insights into trace greenhouse gases during past climate states. The combination of these new
393 techniques will allow the paleoclimate community to better quantify biogeochemical feedbacks
394 and climate sensitivity to greenhouse gas forcings across a range of climate states, and ultimately
395 improve climate forecasts for the coming decades to millennia.

396 In summary, the paleoclimate record is the basis for how we understand the potential range
397 and rate of climate change. Past climates represent the only target for climate model predic-
398 tions at CO₂ concentrations outside of the narrow historical range and, for this reason, are vital
399 tools for evaluating the newest generation of Earth system models. The study of past climates
400 continues to reveal key insights to the Earth’s response to elevated concentrations of greenhouse
401 gases. Innovations in Earth system models, geochemical techniques, and statistical methods
402 further allow for a more direct connection from the past to the future – worlds for which the
403 preindustrial and industrial climate states provide limited guidance. The future of paleoclima-
404 tology is to incorporate past climate information formally in model evaluation, so that we can
405 better predict and plan for the impacts of anthropogenic climate change.

Acknowledgements

This paper is an outcome of an Aspen Global Change Institute workshop funded by NASA and the Heising-Simons Foundation. **Funding:** Tierney and Poulsen acknowledge support from grant #2016-015 from the Heising-Simons Foundation. Kirtland-Turner acknowledges support from grant #2015-145 from the Heising-Simons Foundation. **Author contributions:** Authorship of this manuscript is organized into three tiers according to the contributions of each individual author. Tierney, Poulsen, and Montañez (Tier I) organized the concept, structure and writing of the manuscript, contributed to all sections of the text, designed the final figures, and wrote the Review Summary. Tier II authors (listed alphabetically following Montañez) assumed a leading role in the development of different sections of the text as well as the figure design. Tier III authors (listed alphabetically following Zhu) contributed to the text and figure design under the leadership of the other tiers. **Competing interests:** The authors declare that they have no competing interests. **Data and materials availability:** The figures in this Review paper employ data from previously published works with a few exceptions. The scaled temperature record in Fig. 1 follows ref. (104) but extends further back in time; likewise the CO₂ curve in Fig. 1 follows ref. (105) but has been updated with data published since then. The future projections of CO₂ concentrations calculated with cGENIE shown in Fig. 4 were run for this Review paper. All of these data are available for download from <https://github.com/jesstierney/PastClimates>.

References

1. R. Hooke, *The Posthumous Works of Robert Hooke ... Containing His Cutlerian Lectures, and Other Discourses, Read at the Meetings of the Illustrious Royal Society ... Illustrated*

- with Sculptures* (The Royal Society, London, 1705), pp. 342–343.
2. J. Zachos, M. Pagani, L. Sloan, E. Thomas, K. Billups, Trends, Rhythms, and Aberrations in Global Climate 65 Ma to Present. *Science* **292**, 686–693 (2001).
 3. K. D. Burke, *et al.*, Pliocene and Eocene provide best analogs for near-future climates. *Proceedings of the National Academy of Sciences* **115**, 13288–13293 (2018).
 4. G. A. Schmidt, *et al.*, Practice and philosophy of climate model tuning across six US modeling centers. *Geoscientific Model Development* **10**, 3207–3223 (2017).
 5. M. Huber, R. Caballero, The early Eocene equable climate problem revisited. *Climate of the Past* **7**, 603–633 (2011).
 6. V. Lauretano, J. C. Zachos, L. J. Lourens, Orbitally Paced Carbon and Deep-Sea Temperature Changes at the Peak of the Early Eocene Climatic Optimum. *Paleoceanography and Paleoclimatology* **33**, 1050–1065 (2018).
 7. D. A. Hodell, J. E. T. Channell, J. H. Curtis, O. E. Romero, U. Röhl, Onset of “Hudson Strait” Heinrich events in the eastern North Atlantic at the end of the middle Pleistocene transition (~ 640 ka)? *Paleoceanography* **23**, PA4218 (2008).
 8. J. C. Walker, P. Hays, J. F. Kasting, A negative feedback mechanism for the long-term stabilization of Earth’s surface temperature. *Journal of Geophysical Research: Oceans* **86**, 9776–9782 (1981).
 9. B. Bereiter, *et al.*, Revision of the EPICA Dome C CO₂ record from 800 to 600 kyr before present. *Geophysical Research Letters* **42**, 542–549 (2015).
 10. W. Konrad, D. L. Royer, P. J. Franks, A. Roth-Nebelsick, Quantitative critique of leaf-based paleo-CO₂ proxies: Consequences for their reliability and applicability. *Geological Journal* pp. 1–17 (2020).
 11. M. J. Henehan, *et al.*, Rapid ocean acidification and protracted Earth system recovery followed the end-Cretaceous Chicxulub impact. *Proceedings of the National Academy of Sciences* **116**, 22500–22504 (2019).
 12. Y. Godd ris, Y. Donnadi u, G. Le Hir, V. Lefebvre, E. Nardin, The role of palaeogeography in the Phanerozoic history of atmospheric CO₂ and climate. *Earth-Science Reviews* **128**, 122–138 (2014).
 13. J. G. Charney, *et al.*, *Carbon Dioxide and Climate: A Scientific Assessment* (National Academy of Sciences, Washington, DC, 1979).
 14. C. Hope, The 10 trillion value of better information about the transient climate response. *Philosophical Transactions of the Royal Society A: Mathematical, Physical and Engineering Sciences* **373**, 20140429 (2015).

15. M. D. Zelinka, *et al.*, Causes of Higher Climate Sensitivity in CMIP6 Models. *Geophysical Research Letters* **47**, e2019GL085782 (2020).
16. R. Caballero, M. Huber, State-dependent climate sensitivity in past warm climates and its implications for future climate projections. *Proceedings of the National Academy of Sciences* **110**, 14162–14167 (2013).
17. K. Meraner, T. Mauritsen, A. Voigt, Robust increase in equilibrium climate sensitivity under global warming. *Geophysical Research Letters* **40**, 5944–5948 (2013).
18. T. Friedrich, A. Timmermann, M. Tigchelaar, O. E. Timm, A. Ganopolski, Nonlinear climate sensitivity and its implications for future greenhouse warming. *Science Advances* **2**, e1501923 (2016).
19. J. Zhu, C. J. Poulsen, J. E. Tierney, Simulation of Eocene extreme warmth and high climate sensitivity through cloud feedbacks. *Science Advances* **5**, eaax1874 (2019).
20. C. S. Bretherton, Insights into low-latitude cloud feedbacks from high-resolution models. *Philosophical Transactions of the Royal Society A: Mathematical, Physical and Engineering Sciences* **373**, 20140415 (2015).
21. T. Schneider, C. M. Kaul, K. G. Pressel, Possible climate transitions from breakup of stratocumulus decks under greenhouse warming. *Nature Geoscience* **12**, 163–167 (2019).
22. D. J. Lunt, *et al.*, DeepMIP: Model intercomparison of early Eocene climatic optimum (EECO) large-scale climate features and comparison with proxy data. *Climate of the Past Discussions* pp. 1–27 (2020).
23. J. Zhu, C. J. Poulsen, B. L. Otto-Bliesner, High climate sensitivity in CMIP6 model not supported by paleoclimate. *Nature Climate Change* **10**, 378–379 (2020).
24. D. Beerling, A. Fox, D. Stevenson, P. Valdes, Enhanced chemistry-climate feedbacks in past greenhouse worlds. *Proceedings of the National Academy of Sciences* **108**, 9770–9775 (2011).
25. J. L. Bamber, M. Oppenheimer, R. E. Kopp, W. P. Aspinall, R. M. Cooke, Ice sheet contributions to future sea-level rise from structured expert judgment. *Proceedings of the National Academy of Sciences* **116**, 11195–11200 (2019).
26. M. G. Wise, J. A. Dowdeswell, M. Jakobsson, R. D. Larter, Evidence of marine ice-cliff instability in Pine Island Bay from iceberg-keel plough marks. *Nature* **550**, 506–510 (2017).
27. S. Gulick, *et al.*, Initiation and long-term instability of the East Antarctic Ice Sheet. *Nature* **552**, 225–229 (2017).
28. A. Rovere, *et al.*, The analysis of Last Interglacial (MIS 5e) relative sea-level indicators: Reconstructing sea-level in a warmer world. *Earth-Science Reviews* **159**, 404–427 (2016).

29. A. Dutton, *et al.*, Sea-level rise due to polar ice-sheet mass loss during past warm periods. *science* **349**, aaa4019 (2015).
30. J. Austermann, *et al.*, The impact of dynamic topography change on antarctic ice sheet stability during the mid-pliocene warm period. *Geology* **43**, 927–930 (2015).
31. B. P. Horton, R. Kopp, A. Dutton, T. Shaw, Geological records of past sea-level changes as constraints for future projections. *PAGES Magazine* **27**, 28–29 (2019).
32. R. M. DeConto, D. Pollard, Contribution of Antarctica to past and future sea-level rise. *Nature* **531**, 591–597 (2016).
33. T. Edwards, *et al.*, Revisiting Antarctic ice loss due to marine ice-cliff instability. *Nature* **566**, 58–64 (2019).
34. O. A. Dumitru, *et al.*, Constraints on global mean sea level during Pliocene warmth. *Nature* **574**, 233–236 (2019).
35. A. M. Dolan, B. De Boer, J. Bernales, D. J. Hill, A. M. Haywood, High climate model dependency of Pliocene Antarctic ice-sheet predictions. *Nature communications* **9**, 1–12 (2018).
36. E. Gasson, R. M. DeConto, D. Pollard, R. H. Levy, Dynamic Antarctic ice sheet during the early to mid-Miocene. *Proceedings of the National Academy of Sciences* **113**, 3459–3464 (2016).
37. A. J. McMichael, R. E. Woodruff, S. Hales, Climate change and human health: present and future risks. *The Lancet* **367**, 859–869 (2006).
38. R. L. Wilby, A review of climate change impacts on the built environment. *Built Environment* **33**, 31–45 (2007).
39. A. Arneth, *et al.*, Terrestrial biogeochemical feedbacks in the climate system. *Nature Geoscience* **3**, 525–532 (2010).
40. R. Knutti, J. Sedláček, Robustness and uncertainties in the new CMIP5 climate model projections. *Nature Climate Change* **3**, 369 (2013).
41. C. Deser, A. Phillips, V. Bourdette, H. Teng, Uncertainty in climate change projections: the role of internal variability. *Climate Dynamics* **38**, 527–546 (2012).
42. PAGES Hydro2k Consortium, Comparing proxy and model estimates of hydroclimate variability and change over the Common Era. *Climate of the Past* **13**, 1851–1900 (2017).
43. L. C. Ivany, *et al.*, Intra-annual isotopic variation in *Venericardia* bivalves: implications for early Eocene temperature, seasonality, and salinity on the US Gulf Coast. *Journal of Sedimentary Research* **74**, 7–19 (2004).
44. C. R. Keating-Bitonti, L. C. Ivany, H. P. Affek, P. Douglas, S. D. Samson, Warm, not super-hot, temperatures in the early Eocene subtropics. *Geology* **39**, 771–774 (2011).

45. K. Thirumalai, P. N. DiNezio, J. E. Tierney, M. Puy, M. Mohtadi, An El Niño Mode in the Glacial Indian Ocean? *Paleoceanography and Paleoclimatology* **34**, 1316–1327 (2019).
46. H. L. Ford, A. C. Ravelo, P. J. Polissar, Reduced El Niño–Southern Oscillation during the Last Glacial Maximum. *Science* **347**, 255–258 (2015).
47. A. Frappier, T. Knutson, K.-B. Liu, K. Emanuel, Perspective: Coordinating paleoclimate research on tropical cyclones with hurricane-climate theory and modelling. *Tellus A: Dynamic Meteorology and Oceanography* **59**, 529–537 (2007).
48. P. N. DiNezio, J. E. Tierney, The effect of sea level on glacial Indo-Pacific climate. *Nature Geoscience* **6**, 485–491 (2013).
49. I. M. Held, B. J. Soden, Robust responses of the hydrological cycle to global warming. *Journal of Climate* **19**, 5686–5699 (2006).
50. N. J. Burls, A. V. Fedorov, Wetter subtropics in a warmer world: Contrasting past and future hydrological cycles. *Proceedings of the National Academy of Sciences* **114**, 12888–12893 (2017).
51. C. Muller, P. O’Gorman, An energetic perspective on the regional response of precipitation to climate change. *Nature Climate Change* **1**, 266–271 (2011).
52. M. P. Byrne, P. A. O’Gorman, The response of precipitation minus evapotranspiration to climate warming: Why the “wet-get-wetter, dry-get-drier” scaling does not hold over land. *Journal of Climate* **28**, 8078–8092 (2015).
53. M. P. Byrne, P. A. O’Gorman, Trends in continental temperature and humidity directly linked to ocean warming. *Proceedings of the National Academy of Sciences* **115**, 4863–4868 (2018).
54. E. Erfani, N. J. Burls, The Strength of Low-Cloud Feedbacks and Tropical Climate: A CESM Sensitivity Study. *Journal of Climate* **32**, 2497–2516 (2019).
55. S. Bony, *et al.*, Clouds, circulation and climate sensitivity. *Nature Geoscience* **8**, 261–268 (2015).
56. P. N. DiNezio, *et al.*, Glacial changes in tropical climate amplified by the Indian Ocean. *Science Advances* **4**, eaat9658 (2018).
57. J. E. Tierney, F. S. Pausata, P. B. deMenocal, Rainfall regimes of the Green Sahara. *Science Advances* **3**, e1601503 (2017).
58. W. R. Boos, R. L. Korty, Regional energy budget control of the intertropical convergence zone and application to mid-holocene rainfall. *Nature Geoscience* **9**, 892–897 (2016).
59. P. Ceppi, G. Zappa, T. G. Shepherd, J. M. Gregory, Fast and slow components of the extratropical atmospheric circulation response to CO₂ forcing. *Journal of Climate* **31**, 1091–1105 (2018).

60. J. K. Sniderman, *et al.*, Southern Hemisphere subtropical drying as a transient response to warming. *Nature Climate Change* **9**, 232–236 (2019).
61. R. Feng, C. J. Poulsen, M. Werner, Tropical circulation intensification and tectonic extension recorded by Neogene terrestrial $\delta^{18}\text{O}$ records of the western United States. *Geology* **44**, 971–974 (2016).
62. B. Carrapa, M. Clementz, R. Feng, Ecological and hydroclimate responses to strengthening of the Hadley circulation in South America during the Late Miocene cooling. *Proceedings of the National Academy of Sciences* **116**, 9747–9752 (2019).
63. D. E. Ibarra, *et al.*, Warm and cold wet states in the western United States during the Pliocene–Pleistocene. *Geology* **46**, 355–358 (2018).
64. B. I. Cook, T. R. Ault, J. E. Smerdon, Unprecedented 21st century drought risk in the American Southwest and Central Plains. *Science Advances* **1**, e1400082 (2015).
65. H. C. Jenkyns, Geochemistry of oceanic anoxic events. *Geochemistry, Geophysics, Geosystems* **11**, Q03004 (2010).
66. A. D. Rooney, *et al.*, Re-Os geochronology and coupled Os-Sr isotope constraints on the Sturtian snowball Earth. *Proceedings of the National Academy of Sciences* **111**, 51–56 (2014).
67. R. E. Zeebe, J. C. Zachos, G. R. Dickens, Carbon dioxide forcing alone insufficient to explain Palaeocene–Eocene Thermal Maximum warming. *Nature Geoscience* **2**, 576–580 (2009).
68. M. Gutjahr, *et al.*, Very large release of mostly volcanic carbon during the Palaeocene–Eocene Thermal Maximum. *Nature* **548**, 573–577 (2017).
69. Y. Cui, B. A. Schubert, Atmospheric $p\text{CO}_2$ reconstructed across five early Eocene global warming events. *Earth and Planetary Science Letters* **478**, 225–233 (2017).
70. S. K. Turner, P. M. Hull, L. R. Kump, A. Ridgwell, A probabilistic assessment of the rapidity of PETM onset. *Nature Communications* **8**, 353 (2017).
71. S. K. Turner, Constraints on the onset duration of the Paleocene–Eocene Thermal Maximum. *Philosophical Transactions of the Royal Society A: Mathematical, Physical and Engineering Sciences* **376**, 20170082 (2018).
72. G. N. Inglis, *et al.*, Global mean surface temperature and climate sensitivity of the EECO, PETM and latest Paleocene. *Climate of the Past Discussions* pp. 1–43 (2020).
73. D. E. Penman, B. Hönisch, R. E. Zeebe, E. Thomas, J. C. Zachos, Rapid and sustained surface ocean acidification during the Paleocene–Eocene Thermal Maximum. *Paleoceanography* **29**, 357–369 (2014).

74. J. C. Zachos, *et al.*, Rapid acidification of the ocean during the Paleocene-Eocene thermal maximum. *Science* **308**, 1611–1615 (2005).
75. E. Thomas, N. J. Shackleton, The Paleocene-Eocene benthic foraminiferal extinction and stable isotope anomalies. *Geological Society, London, Special Publications* **101**, 401–441 (1996).
76. M. J. Carmichael, *et al.*, Hydrological and associated biogeochemical consequences of rapid global warming during the Paleocene-Eocene Thermal Maximum. *Global and Planetary Change* **157**, 114–138 (2017).
77. G. J. Bowen, J. C. Zachos, Rapid carbon sequestration at the termination of the Palaeocene–Eocene Thermal Maximum. *Nature Geoscience* **3**, 866 (2010).
78. R. E. Zeebe, A. Ridgwell, J. C. Zachos, Anthropogenic carbon release rate unprecedented during the past 66 million years. *Nature Geoscience* **9**, 325–329 (2016).
79. D. Archer, H. Kheshgi, E. Maier-Reimer, Multiple timescales for neutralization of fossil fuel CO₂. *Geophysical Research Letters* **24**, 405–408 (1997).
80. C. Emiliani, Pleistocene temperatures. *The Journal of Geology* **63**, 538–578 (1955).
81. J. Zhou, C. Poulsen, D. Pollard, T. White, Simulation of modern and middle Cretaceous marine $\delta^{18}\text{O}$ with an ocean-atmosphere GCM. *Paleoceanography* **23**, PA3223 (2008).
82. E. Brady, *et al.*, The connected isotopic water cycle in the Community Earth System Model version 1. *Journal of Advances in Modeling Earth Systems* **11**, 2547–2566 (2019).
83. J. Zhu, *et al.*, Simulation of early Eocene water isotopes using an Earth system model and its implication for past climate reconstruction. *Earth and Planetary Science Letters* **537**, 116164 (2020).
84. M. N. Evans, S. E. Tolwinski-Ward, D. M. Thompson, K. J. Anchukaitis, Applications of proxy system modeling in high resolution paleoclimatology. *Quaternary Science Reviews* **76**, 16–28 (2013).
85. S. Tolwinski-Ward, K. Anchukaitis, M. Evans, Bayesian parameter estimation and interpretation for an intermediate model of tree-ring width. *Climate of the Past* **9**, 1481–1493 (2013).
86. C. N. Jex, S. Phipps, A. Baker, C. Bradley, Reducing uncertainty in the climatic interpretations of speleothem $\delta^{18}\text{O}$. *Geophysical Research Letters* **40**, 2259–2264 (2013).
87. J. E. Tierney, M. P. Tingley, BAYSPLINE: A new calibration for the alkenone paleothermometer. *Paleoceanography and Paleoclimatology* **33**, 281–301 (2018).
88. J. E. Tierney, A. M. Haywood, R. Feng, T. Bhattacharya, B. L. Otto-Bliesner, Pliocene warmth consistent with greenhouse gas forcing. *Geophysical Research Letters* **46**, 9136–9144 (2019).

89. E. C. Gill, B. Rajagopalan, P. Molnar, T. M. Marchitto, Reduced-dimension reconstruction of the equatorial Pacific SST and zonal wind fields over the past 10,000 years using Mg/Ca and alkenone records. *Paleoceanography* **31**, 928–952 (2016).
90. G. J. Hakim, *et al.*, The last millennium climate reanalysis project: Framework and first results. *Journal of Geophysical Research: Atmospheres* **121**, 6745–6764 (2016).
91. J. E. Tierney, *et al.*, Glacial cooling and climate sensitivity revisited. *Nature* p. in press (2020).
92. V. Eyring, *et al.*, Overview of the Coupled Model Intercomparison Project Phase 6 (CMIP6) experimental design and organization. *Geoscientific Model Development* **9**, 1937–1958 (2016).
93. G. Schmidt, *et al.*, Using palaeo-climate comparisons to constrain future projections in CMIP5. *Climate of the Past* **10**, 221–250 (2013).
94. I. M. Held, The gap between simulation and understanding in climate modeling. *Bulletin of the American Meteorological Society* **86**, 1609–1614 (2005).
95. J. D. White, *et al.*, A process-based ecosystem model (Paleo-BGC) to simulate the dynamic response of late Carboniferous plants to Variable CO₂, Elevated O₂ and Aridification. *American Journal of Science* (in press).
96. G. Damour, T. Simonneau, H. Cochard, L. Urban, An overview of models of stomatal conductance at the leaf level. *Plant, Cell & Environment* **33**, 1419–1438 (2010).
97. S. Hoetzel, L. Dupont, E. Schefuß, F. Rommerskirchen, G. Wefer, The role of fire in Miocene to Pliocene C₄ grassland and ecosystem evolution. *Nature Geoscience* **6**, 1027–1030 (2013).
98. B. H. Lomax, *et al.*, Plant spore walls as a record of long-term changes in ultraviolet-B radiation. *Nature Geoscience* **1**, 592 (2008).
99. S. Schüpbach, *et al.*, Greenland records of aerosol source and atmospheric lifetime changes from the Eemian to the Holocene. *Nature Communications* **9**, 1476 (2018).
100. S. Kienast, G. Winckler, J. Lippold, S. Albani, N. Mahowald, Tracing dust input to the global ocean using thorium isotopes in marine sediments: Thoromap. *Global Biogeochemical Cycles* **30**, 1526–1541 (2016).
101. J. H. Seinfeld, *et al.*, Improving our fundamental understanding of the role of aerosol-cloud interactions in the climate system. *Proceedings of the National Academy of Sciences* **113**, 5781–5790 (2016).
102. G. N. Inglis, *et al.*, $\delta^{13}\text{C}$ values of bacterial hopanoids and leaf waxes as tracers for methanotrophy in peatlands. *Geochimica et Cosmochimica Acta* **260**, 244–256 (2019).
103. Y. G. Zhang, M. Pagani, J. Henderiks, H. Ren, A long history of equatorial deep-water upwelling in the Pacific Ocean. *Earth and Planetary Science Letters* **467**, 1–9 (2017).

104. J. Hansen, M. Sato, G. Russell, P. Kharecha, Climate sensitivity, sea level and atmospheric carbon dioxide. *Philosophical Transactions of the Royal Society A: Mathematical, Physical and Engineering Sciences* **371**, 20120294–20120294 (2013).
105. G. L. Foster, D. L. Royer, D. J. Lunt, Future climate forcing potentially without precedent in the last 420 million years. *Nature Communications* **8**, 14845 (2017).
106. O. Friedrich, R. D. Norris, J. Erbacher, Evolution of middle to Late Cretaceous oceans – a 55 my record of Earth’s temperature and carbon cycle. *Geology* **40**, 107–110 (2012).
107. C. R. Witkowski, J. W. Weijers, B. Blais, S. Schouten, J. S. S. Damsté, Molecular fossils from phytoplankton reveal secular $p\text{CO}_2$ trend over the Phanerozoic. *Science Advances* **4**, eaat4556 (2018).
108. S. M. Soshian, *et al.*, Constraining the evolution of Neogene ocean carbonate chemistry using the boron isotope pH proxy. *Earth and Planetary Science Letters* **498**, 362–376 (2018).
109. M. Meinshausen, *et al.*, The SSP greenhouse gas concentrations and their extensions to 2500. *Geoscientific Model Development Discussions* **2019**, 1–77 (2019).
110. E. L. Grossman, T.-L. Ku, Oxygen and carbon isotope fractionation in biogenic aragonite: Temperature effects. *Chemical Geology* **59**, 59–74 (1986).
111. J. Zhu, *et al.*, Reduced ENSO variability at the LGM revealed by an isotope-enabled Earth system model. *Geophysical Research Letters* **44**, 6984–6992 (2017).
112. R. M. DeConto, *et al.*, Thresholds for Cenozoic bipolar glaciation. *Nature* **455**, 652–656 (2008).

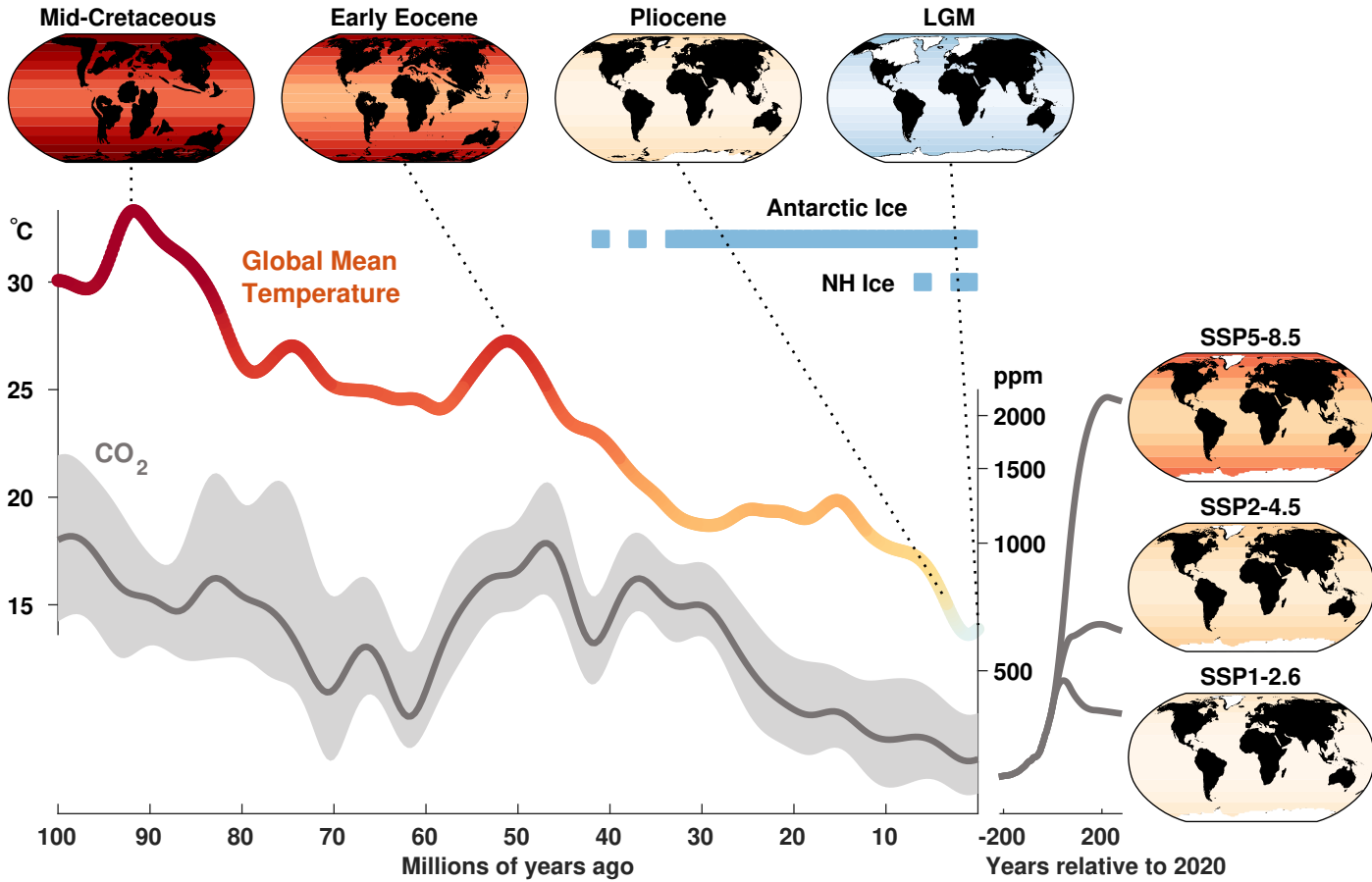


Figure 1: **Paleoclimate context for future climate scenarios.** Global mean surface temperature for the past 100 million years is estimated from benthic $\delta^{18}\text{O}$ (2, 106) using the method of (104). CO_2 is estimated from the multi-proxy data set compiled by (105) with additional phytane data from (107) and boron data from (108) and (11). Data with unrealistic values (<150 ppm) are excluded. The CO_2 error envelopes represent 1σ uncertainties. Note logarithmic scale for CO_2 . Gaussian smoothing was applied to both the temperature and CO_2 curves in order to emphasize long-term trends. Temperature colors are scaled relative to preindustrial conditions. The maps show simplified representations of surface temperature. Projected CO_2 concentrations are from the extended SSP scenarios (109). Blue bars indicate when there are well-developed ice sheets (solid lines) and intermittent ice sheets (dashed lines), according to previous syntheses (2).

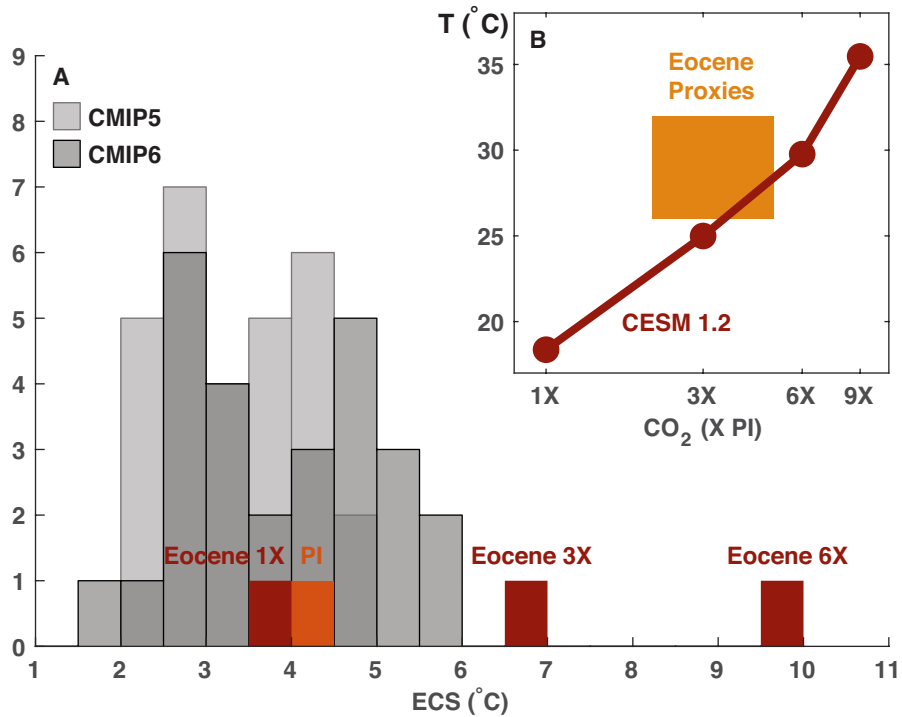


Figure 2: **Constraining equilibrium climate sensitivity (ECS) through simulation of the early Eocene.** a. ECS in CMIP5 and CMIP6 models (grey bars; (15)) compared to ECS in the CESM1.2 preindustrial (PI, orange bar) and Eocene simulations with 1X, 3X and 6X preindustrial CO₂ levels (red bars). b. CO₂ concentrations (times preindustrial level) vs. global mean temperature according to early Eocene proxies (yellow patch) compared to the results from the CESM1.2 Eocene simulations. Proxy CO₂ estimates are a 2 σ range derived from the collection plotted in Figure 1. Readers are referred to (19) for details of the Eocene climate simulations and proxy global mean temperature estimation.

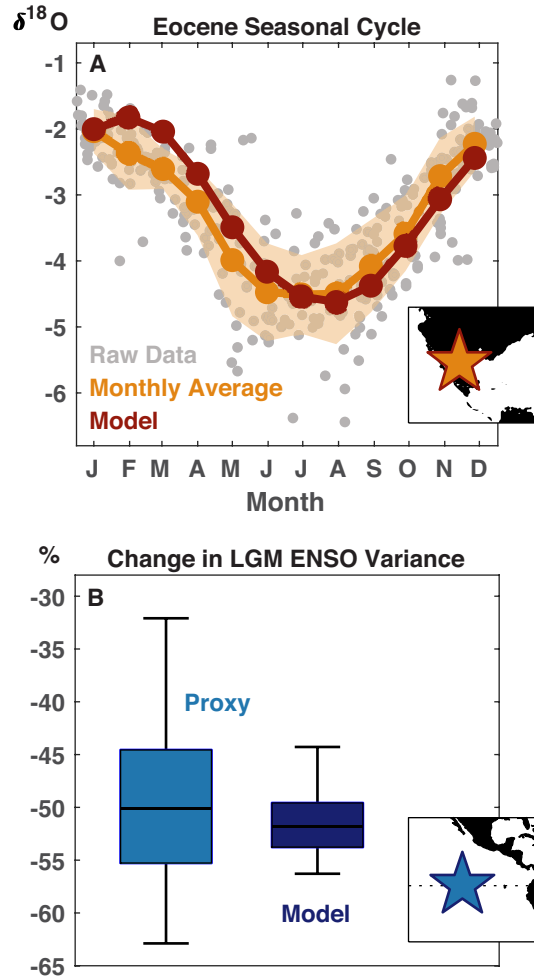


Figure 3: **Examples of seasonal and interannual paleoclimate data and comparison to models.** (a) Seasonally-resolved $\delta^{18}\text{O}$ carbonate from the shells of a fossil bivalve, *Venericardia hatcheplata*, from the early Eocene Hatchetigbee Formation (orange star in inset) (43, 44). Monthly averaged data (orange, with 1σ uncertainty bounds) are compared with predicted $\delta^{18}\text{O}$ -carbonate seasonality at the same grid-point from an isotope-enabled Eocene model simulation (19) (red) (using modeled $\delta^{18}\text{O}$ of seawater and SST, and the calibration of ref. (110)). (b) Mg/Ca measurements of individual planktic foraminifera *Trilobatus sacculifer* from an eastern equatorial site (blue star in inset) provide proxy evidence of a reduction in ENSO variability during the Last Glacial Maximum (LGM) relative to pre-industrial conditions (46) (lighter blue). The magnitude of reduction agrees with simulations using CESM1.2 (darker blue) (111).

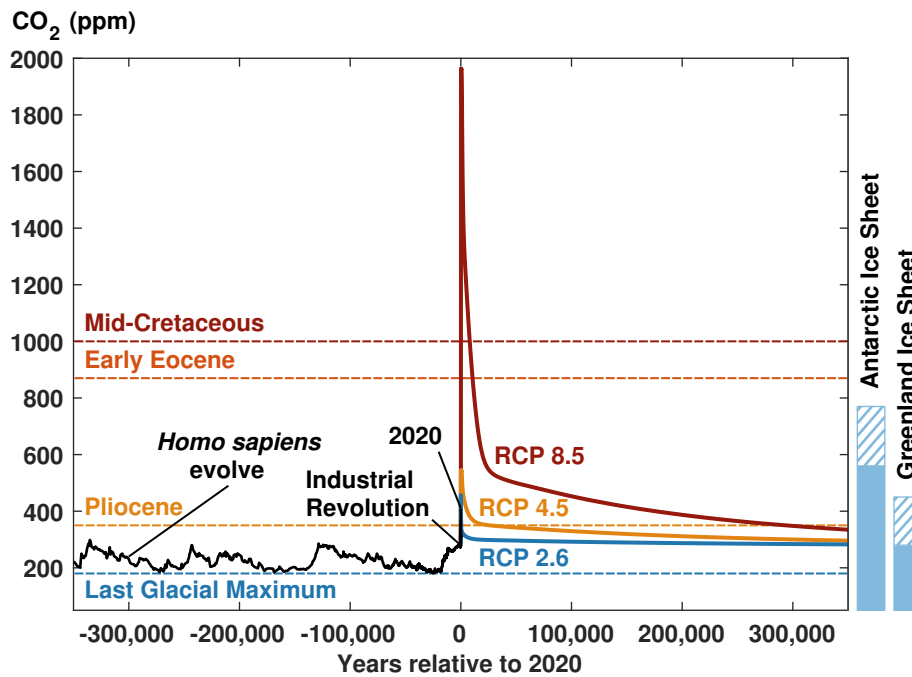


Figure 4: **The anthropogenic climate aberration.** Black line shows CO₂ measured in ice cores for the past 350,000 years (9). Solid colored lines show future CO₂ concentrations for the IPCC AR5 Representative Concentration Pathways, run out to 350,000 years in the future with the cGENIE model. Dotted lines indicate average CO₂ for key time periods in the geologic past. Bars at right indicate CO₂ concentrations under which there are well-developed ice sheets (solid areas) and intermittent ice sheets (hatched areas), based on geologic evidence and ice sheet modeling (112).

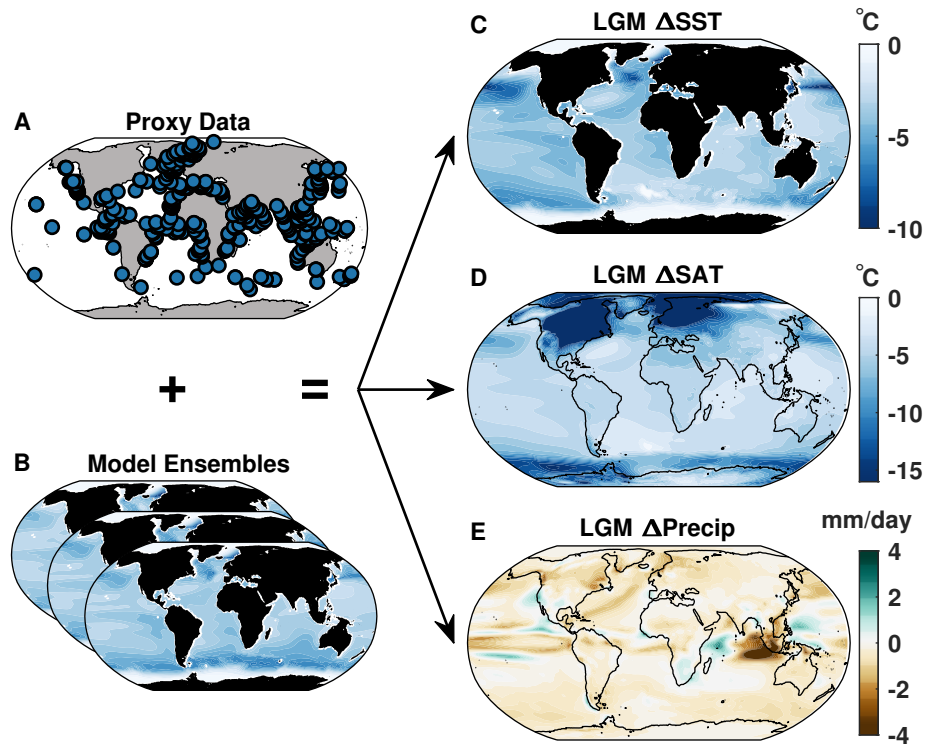


Figure 5: **An example of paleoclimate data assimilation.** Marine sea-surface temperature (SST) proxy data from the Last Glacial Maximum (LGM) and the Late Holocene (a) are combined with an ensemble of model simulations (b) which contain multiple climatic variables. The results (c-e; LGM - Late Holocene differences for sea-surface temperature (Δ SST), surface air temperature (Δ SAT), and mean annual precipitation (Δ Precip)) include all the variables in the model prior, which are influenced by the assimilated SST proxy data. Proxy data, model fields, and assimilated results are from ref. (91).